JACS
JOURNAL OF THE AMERICAN CHEMICAL SOCIETY
Communication
pubs.acs.org/JACS

Development of Composite Inorganic Building Blocks for MOFs

Shou-Tian Zheng,[†] Tao Wu,[‡] Chengtsung Chou,[†] Addis Fuhr,[†] Pingyun Feng,*[,‡] and Xianhui Bu*[,†]

[†]Department of Chemistry and Biochemistry, California State University, Long Beach, California 90840, United States
[‡]Department of Chemistry, University of California, Riverside, California 92521, United States

Supporting Information

ABSTRACT: A general direction for diversifying metal−organic frameworks (MOFs) is demonstrated by the synthesis of composite inorganic clusters between indium and s-, d-, and f-block elements. These previously unknown heterometallic clusters, with various nuclearity, geometry, charge, and metal-to-metal ratios, significantly expand the pool of inorganic building blocks that are highly effective for the construction of porous MOFs with high gas uptake capacity.

Crystalline porous materials (CPMs) comprise a broad range of solid-state materials with diverse compositions, structures, and properties.[1−7] Metal−organic framework (MOF) materials are the most recent addition to this family.[1−5] In the past decade, many advances in MOFs have been made due to the availability of a practically infinite number of organic building blocks. In comparison, much fewer inorganic building blocks are currently known.

One of the most promising routes to increase the number of inorganic components should be the creation of composite inorganic building units, because given dozens of chemical elements, the number of different ways to combine them (in various ratios) is just as large as the types of organic molecules. Here we focus on two general approaches that could greatly increase the diversity of inorganic building blocks. The first is the integration (in the same material) of two or more elements that were not known to co-exist (in 3D MOFs) prior to our work. For example, indium is rarely known to form 3D MOFs with other types of elements, such as Mg, Mn, Co, Cu, and lanthanide (Ln) ions, even though each of these individual elements is well known as a building block for MOFs.

The second approach involves the creation of composite inorganic clusters as framework building blocks. This has remained a significant challenge in MOF chemistry, because a common occurrence in attempts to synthesize heterometallic MOFs is the *macroscopic phase separation* of different metal ions into separate phases or the *molecular-level separation* of such metal ions by organic ligands.[8−10] Prior to this work, heterometallic MOFs, especially those based on the combination of d- and f-block elements, were already well known.[8] However, there have been much fewer examples in which heterometallic metals combine to form discrete clusters cross-linkable by organic ligands into 3D MOFs.[11]

Herein, we report five series of MOFs, CPM-18-M (M = Nd, Sm), CPM-19-M (M = Nd, Pr), CPM-20, CPM-21-M (M = Mn, Co, Cu), and CPM-23, based on indium heterometallic clusters (Table 1). For the first time, the p-block indium is shown to be capable of co-assembling with metals from any other block of the periodic table to afford a pool of new heterometallic clusters for fabricating MOFs. These In-M clusters possess diverse configuration, nuclearity, metal-to-metal ratio, and charge, as shown by trimeric $[InCo_2(OH)]^{6+}$, tetrameric *trans*-$[In_2M_2(OH)_2]^{8+}$ (M = Mn, Co, Cu), tetrameric *cis*-$[In_2Mg_2(OH)_2]^{8+}$, tetrameric cube-$[In_3M(OH)_4]^{8+}$ (M = Nd, Sm), and pentameric $[In_3M_2(OH)_3O]^{10+}$ (M = Nd, Pr) (Figure 1). To our knowledge, with the exception of tetrameric *trans*-$[In_2M_2(OH)_2]^{8+}$, which is known in isolated In-M heterometallic complexes, no other In-M heterometallic oxide clusters have been known prior to this work.[12] One factor that increases the variety of such clusters is that, for the same nuclearity, the ratio between heterometals can have different values (e.g., 3:1 or 2:2 for tetramers). Even though these clusters look quite different from each other, there appears to be an intrinsic relationship among them, because the overall charge of each cluster is exactly twice its nuclearity.

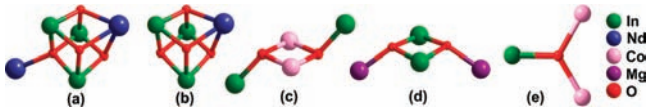

Figure 1. Five types of indium-containing clusters synthesized in this work: (a) $In_3Nd_2(OH)_3O$, (b) $In_3Nd(OH)_4$, (c) *trans*-$In_2Co_2(OH)_2$, (d) *cis*-$In_2Mg_2(OH)_2$, and (e) $InCo_2(OH)$.

CPM-18-Nd contains cubane-like 3:1 $[In_3Nd(OH)_4]^{8+}$ clusters and crystallizes in chiral space group $P2_13$ with three types of cages (Figure 2b−d). Two are constructed from the cross-linking of 4 $[In_3Nd(OH)_4]^{8+}$ clusters by BTCs to form tetrahedral cages with maximum free diameters of ∼6.2 and ∼6.6 Å, while the third is composed of 6 cubane clusters bridged by BTCs to form an octahedral cage with a maximum free diameter of ∼4.2 Å. The sharing of cubane clusters by adjacent cages leads to an overall anionic 3D framework (Figures S1, S2).

In CPM-18-Nd, each $[In_3Nd(OH)_4]^{8+}$ cube coordinates with nine carboxyl groups from nine BTC ligands (Figure S3). Of the nine carboxyl groups, three adopt a bidentate mode by bridging a 6-coordinate In^{3+} ion and a 9-coordinate Nd^{3+} ion, while the remaining six coordinate to only one In^{3+} ion in a monodentate fashion, leaving one uncoordinated oxygen atom per carboxyl group (Figure 2a). As shown below by CPM-19-Nd, these uncoordinated oxygen atoms can bond with

Received: December 19, 2011
Published: February 27, 2012

   dx.doi.org/10.1021/ja2118255 | *J. Am. Chem. Soc.* 2012, 134, 4517−4520

Table 1. Summary of Crystal Data and Refinement Results[a]

name	formula	space group	a/b (Å)	c (Å)	α/β (°)	γ (°)	R(F)
CPM-18-Nd	$[(CH_3)_2NH_2][In_3Nd(OH)_4(BTC)_3(DMF)_3]$·solvent	$P2_13$	16.8753(13)	16.8753(13)	90	90	0.0531
CPM-18-Sm	$[(CH_3)_2NH_2][In_3Sm(OH)_4(BTC)_3(DMF)_3]$·solvent	$P2_13$	16.8845(2)	16.8845(2)	90	90	0.0360
CPM-19-Nd	$[In_3Nd_2O(OH)_3(BTB)_3(H_2O)_6]\cdot NO_3$·solvent	$P2_13$	27.1319(3)	27.1319(3)	90	90	0.0772
CPM-19-Pr	$[In_3Pr_2O(OH)_3(BTB)_3(H_2O)_6]\cdot NO_3$·solvent	$P2_13$	27.1344(1)	27.1344(1)	90	90	0.0465
CPM-20	$[InCo_2(OH)(INA)_3(1,4\text{-}BDC)_{3/2}]$·solvent	$I\bar{4}3m$	21.9141(9)	21.9141(9)	90	90	0.0571
CPM-21-Mn	$[In_2Mn_2(OH)_2(BTB)_{8/3}(DMA)_2]$·solvent	$R\bar{3}$	36.4998(4)	24.1865(7)	90	120	0.0660
CPM-21-Co	$[In_2Co_2(OH)_2(BTB)_{8/3}(DMF)_2]$·solvent	$R\bar{3}$	36.3966(5)	23.9655(6)	90	120	0.0850
CPM-21-Cu	$[In_2Cu_2(OH)_2(BTB)_{8/3}(H_2O)_2]$·solvent	$R\bar{3}$	36.2180(14)	23.6120(19)	90	120	0.0921
CPM-23	$[In_2Mg_2(OH)_2(BTB)_{8/3}(H_2O)_4]$·solvent	$R\bar{3}$	32.2214(3)	92.4420(20)	90	120	0.0433

[a] H_3BTC, trimesic acid; H_3BTB, 1,3,5-tri(4-carboxyphenyl)benzene; HINA, isonicotinic acid; 1,4-H_2BDC, 1,4-benzenedicarboxylic acid.

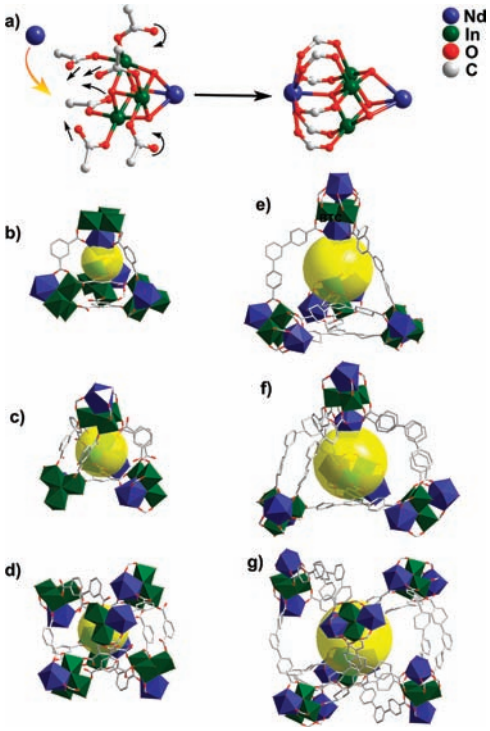

Figure 2. Structural correlation between CPM-18 (left column) and CPM-19 (right column). (a) Some carboxyl groups in CPM-18-Nd contain dangling oxygen atoms that cooperatively grab onto one lanthanide ion in CPM-19-Nd, leading to a change from tetrameric $[In_3Nd(OH)_4]^{8+}$ in CPM-18-Nd to pentameric $[In_3Nd_2(OH)_3O]^{10+}$ in CPM-19-Nd, and a switch from negative to positive framework. Below are three types of polyhedral cages in CPM-18-Nd (b–d) and CPM-19-Nd (e–g).

additional metal ions to form new heterometallic clusters with higher nuclearity.

The structural correlation between CPM-18-Nd and CPM-19-Nd involves the cooperative action of 6 carboxyl groups to capture an additional Ln^{3+} to form a pentamer (Figure 2a). Unlike the $[In_3Nd(OH)_4]^{8+}$ cubes in CPM-18-Nd, CPM-19-Nd is constructed from pentameric $[In_3Nd_2(OH)_3O]^{10+}$ clusters which can be derived from cubane-like clusters by attaching an additional Nd^{3+} ion to one corner of the cube (Figure 2a). Because of the larger size of BTB, the free diameters of two tetrahedral cages and one octahedral cage in CPM-19-Nd are increased to 7.4, 7.6, and 9.4 Å, and the guest-accessible volume (72.8%) of CPM-19-Nd is also larger than that of CPM-18-Nd (41.3%).[13]

One of the most interesting features demonstrated by CPM-18-Nd and CPM-19-Nd is the charge reversal of the framework. By incorporating additional Nd^{3+} cations, CPM-19-Nd adopts an overall cationic framework, in contrast to isoreticular CPM-18-Nd that has an anionic framework. Such a charge reversal among isoreticular MOFs is quite unusual and demonstrates a new mechanism for altering framework charge properties by inserting or removing metal ions in a crystallographically ordered fashion.

In addition to In-Ln clusters shown above, co-assembly of In^{3+} with Co^{2+} gives two types of In-Co clusters of different nuclearity: trimeric $[InCo_2(OH)]^{6+}$ in CPM-20 and tetrameric $[In_2Co_2(OH)_2]^{8+}$ in CPM-21-Co (Figure 1c,e). CPM-20 is both a mixed-metal and mixed-ligand MOF. Trinuclear $[InCo_2(OH)]^{6+}$ clusters in CPM-20 are cross-linked by 6 1,4-BDC ligands and 3 INA ligands to form a nine-connected net with the known ncb topology (Figure S4),[6c,d] having two types of polyhedral cages: tetrahedral $\{[InCo_2(OH)]_4(1,4\text{-}BDC)_6\}$ and square antiprismatic $\{[InCo_2(OH)]_8(INA)_{12}(1,4\text{-}BDC)_2\}$ (Figure 3).

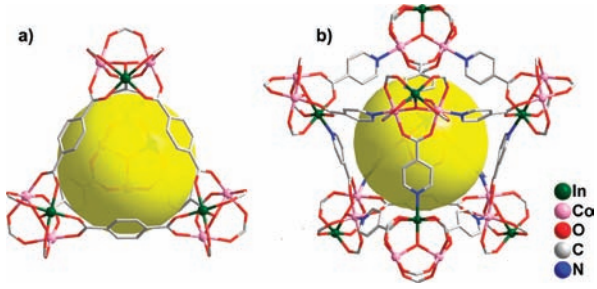

Figure 3. Two types of polyhedral cages in CPM-20.

Unlike the cube-like tetramer in CPM-18-Nd, the chair-like $[In_2Co_2(OH)_2]^{8+}$ tetramer in CPM-21-Co is derived by attaching an additional In^{3+} to the trimeric $InCo_2(OH)$. One likely reason for the different geometries between cube-type In-Ln tetramers and chair-like Ln-Co tetramers is that fewer OH^- groups are needed for the formation of M^{3+}/M^{2+} tetramers (2 OH^- groups) compared to the formation of M^{3+}/M^{3+} tetramers (4 OH^- groups), likely as a result of the lower Co^{2+} charge. The $[In_2Co_2(OH)_2]^{8+}$ tetramer is called *trans* because its 2 In^{3+} ions are oriented in a *trans* fashion with respect to the $\{Co_2(OH)_2\}$ plane. In addition to cobalt, other 3d metals such as Mn and Cu can also form the same *trans* tetramer (Table 1).

The 3D framework in CPM-21-Co is built from simple cubic packing of large octahedral cages $\{[In_2Co_2(OH)_2]_6(BTB)_8\}$

dx.doi.org/10.1021/ja2118255 | J. Am. Chem. Soc. 2012, 134, 4517–4520

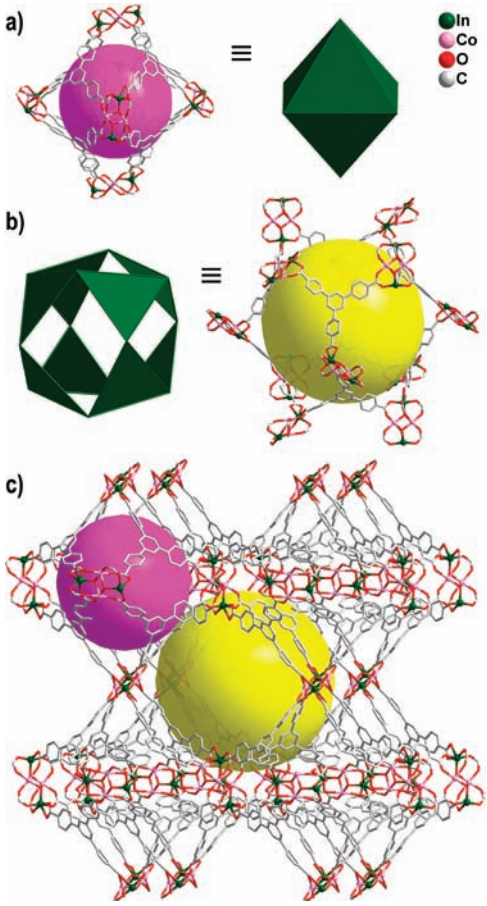

Figure 4. Two types of polyhedral cages in CPM-21-Co (a,b) and its 3D framework (c).

(Figure 4a,c) containing 12 In^{3+} and 12 M^{2+} sites. At each corner of the octahedral cage is a tetrameric *trans*-$[In_2Co_2(OH)_2]^{8+}$ cluster, and 8 BTB ligands occupy the trigonal planes. The inner free diameter of these cages is ~15.5 Å. Furthermore, 8 octahedra enclose a large cuboctahedral cage with a free diameter of ~22.5 Å (Figure 4b). Such an open net, however, results in the formation of a 2-fold interweaving structure. Nevertheless, the overall structure is still quite open, with a total guest-accessible volume of 60.4%.

In addition to the In-Ln (the p-f combinations) and In-Co/Mn/Cu (the p-d combinations) clusters, the first In-Mg (the p-s combination) cluster has also been created. As shown in Figure 1d, $[In_2Mg_2(OH)_2]^{8+}$ clusters in CPM-23 can be viewed as formed by fusing 2 $[In_2Mg(OH)]^{7+}$ trimers sharing the In...In edge, in contrast to *trans*-$[In_2Co_2(OH)_2]^{8+}$ clusters which can be considered as formed by fusing 2 $[InCo_2(OH)]^{6+}$ trimers sharing the Co...Co edge. The $[In_2Mg_2(OH)_2]^{8+}$ cluster is further different from the *trans*-$[In_2Co_2(OH)_2]^{8+}$ cluster because 2 Mg^{2+} ions are oriented in a *cis* fashion with respect to the central $\{In_2(OH)_2\}$ plane.

In CPM-23, every *cis*-$[In_2Mg_2(OH)_2]^{8+}$ cluster is connected by 8 BTB ligands to generate a 3D framework. CPM-23 possesses a high solvent-accessible volume (74.7%). As shown in Figure 5, the accessible volume in the hexagonal channels is delimited by BTB ligands into two individual cavities with internal free diameters of ~10.2 and ~19.5 Å. Both of these cavities can be simplified as octahedral by considering *cis*-$[In_2Mg_2(OH)_2]^{8+}$ clusters as nodes.

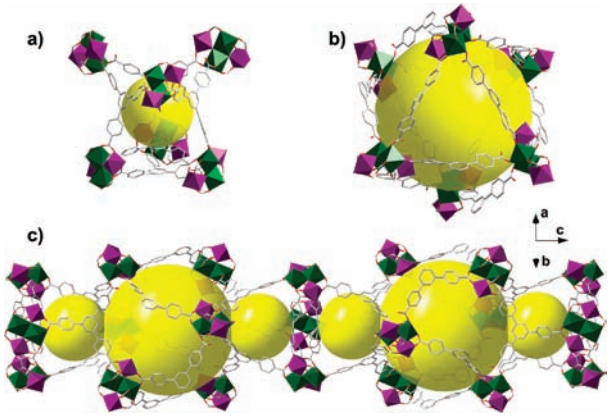

Figure 5. Two types of octahedral cages in CPM-23 (a,b) and side view of 1D hexagonal pattern of CPM-23 along the *c*-axis (c).

Thermogravimetric analyses of CPM-19-Nd and CPM-20 show that removal of solvent molecules occurs at temperatures of 30−150 and 40−300 °C, respectively (Figure S5). PXRD further confirms that CPM-19-Nd and CPM-20 retain their crystallinity up to ~200 and 300 °C (Figures S6, S7), respectively. Thus, CPM-19-Nd and CPM-20 were degassed at 150 and 260 °C, respectively, for 24 h under vacuum prior to the measurement. As shown in Figures 6 and S8, the N_2

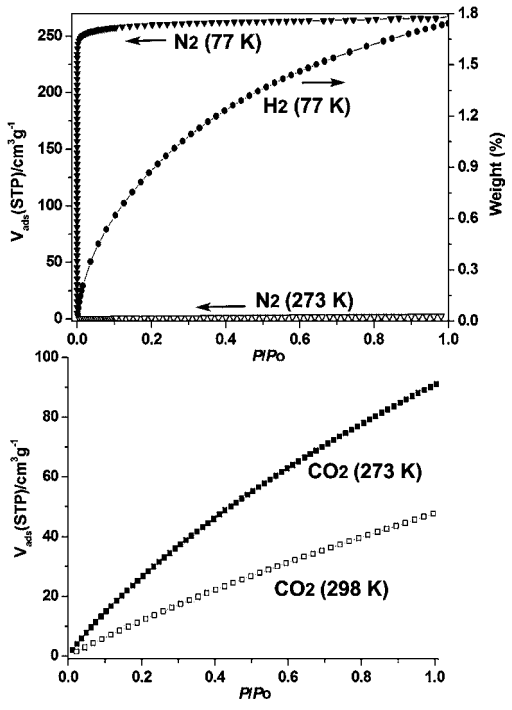

Figure 6. Gas adsorption isotherms of CPM-20.

sorptions of both samples exhibit type I isotherm behavior, typical of materials with permanent microporosity. The BET and Langmuir surface areas of CPM-19-Nd are 272 and 370 m^2/g, respectively. A micropore volume of 0.133 cm^3/g (using Horvath−Kawazoe method) and median pore size of 9.38 Å were calculated. CPM-19-Nd can also adsorb a considerable amount of H_2 at 77 K and 1 atm (1.32 wt%, 6.60 mmol/g), comparable with the highly porous framework ZIFs (ZIF-8, 1.29 wt%, ZIF-11, 1.37 wt%, ZIF-20, 1.1 wt%).[14] Its CO_2 uptake reaches 38.4 cm^3/g at 273 K and 1 atm.

dx.doi.org/10.1021/ja2118255 | J. Am. Chem. Soc. 2012, 134, 4517−4520

Compared to CPM-19-Nd, CPM-20 exhibits significantly higher BET surface area (1009 m^2/g), Langmuir surface area (1134 m^2/g), micropore volume (0.404 cm^3/g), and H_2 uptake at 77 K and 1 atm (195.4 cm^3/g, 1.74 wt%). Furthermore, CPM-20 exhibits very high CO_2 uptake at 273 K and 1 atm (91.2 cm^3/g) and at 298 K and 1 atm (47.7 cm^3/g). The higher uptake of CPM-20 may be due to its lack of extra-framework charge-balancing species. Even though numerous MOF structures have been reported, MOFs with CO_2 uptake >90 cm^3/g at 273 K and 1 atm are still scarce. Further N_2 sorption of CPM-20 at 273 K indicates little uptake over the entire pressure range (2.28 cm^3/g at 1 atm). The selectivity for CO_2/N_2 at 273 K is calculated to be 49:1 at 0.16 atm and 40:1 at 1 atm (or 77:1 at 0.16 atm and 63:1 at 1 atm by weight), indicating CPM-20 has a high CO_2/N_2 selective adsorption.[15]

In summary, with the creation of a large family of MOFs, we have demonstrated the feasibility of and a general direction for greatly diversifying MOFs. A p-block element (indium here) can be co-assembled with elements from any other block of the periodic table (s-, d-, and f-blocks) to create a series of previously unknown composite inorganic building blocks with differing nuclearity (3−5), metal-to-metal ratios (i.e., 2:1, 3:1, 2:2, 3:2), geometry, and charge. These composite inorganic clusters, which are still quite rare among known MOFs, significantly expand the pool of inorganic building blocks and are clearly useful for the construction of porous MOFs with high gas uptake capacity.

■ ASSOCIATED CONTENT

Supporting Information

Details about sample preparation, TGA, XRD, CIF files, and additional structural figures. This material is available free of charge via the Internet at http://pubs.acs.org.

■ AUTHOR INFORMATION

Corresponding Author

xbu@csulb.edu; pingyun.feng@ucr.edu

Notes

The authors declare no competing financial interest.

■ ACKNOWLEDGMENTS

This work was supported by the Department of Energy-Basic Energy Sciences under Contract No. DE-SC0002235 (P.F.), by the NSF (DMR-0846958, X.B.), and by a CSULB SCAC Award.

■ REFERENCES

(1) (a) Chen, B.; Liang, C.; Yang, J.; Contreras, D. S.; Clancy, Y. L.; Lobkovsky, E. B.; Yaghi, O. M.; Dai, S. *Angew. Chem., Int. Ed.* **2006**, *45*, 1390. (b) Farha, O. K.; Hupp, J. T. *Acc. Chem. Res.* **2010**, *43*, 1166. (c) Shultz, A.; Sarjeant, A.; Farha, O.; Hupp, J. T.; Nguyen, S. *J. Am. Chem. Soc.* **2011**, *133*, 13252. (d) Tanabe, K. K.; Cohen, S. M. *Chem. Soc. Rev.* **2011**, *40*, 498.

(2) (a) Li, J. R.; Zhou, H. C. *Nat. Chem.* **2010**, *2*, 893. (b) Pramanik, S.; Zheng, C.; Emge, T. J.; Li, J. *J. Am. Chem. Soc.* **2011**, *133*, 4153. (c) Colombo, V.; Galli, S.; Choi, H. J.; Han, G. D.; Maspero, A.; Palmisano, G.; Masciocchi, N.; Long, J. R. *Chem. Sci.* **2011**, *2*, 1311. (d) He, Y.; Xiang, S.; Chen, B. *J. Am. Chem. Soc.* **2011**, *133*, 14570.

(3) (a) Parnham, E. R.; Morris, R. E. *Acc. Chem. Res.* **2007**, *40*, 1005. (b) Xiao, B.; Byrne, P. J.; Wheatley, P. S.; Wragg, D. S.; Zhao, X. B.; Fletcher, A. J.; Thomas, K. M.; Peters, L.; Evans, J. S. O.; Warren, J. E.; Zhou, W. Z.; Morris, R. E. *Nat. Chem.* **2009**, *1*, 289. (c) Koh, K.; Wong-Foy, A. G.; Matzger, A. J. *J. Am. Chem. Soc.* **2010**, *132*, 15005.

(4) Cairns, A. J.; Perman, J. A.; Wojtas, L.; Kravtsov, V. C.; Alkordi, M. E.; Zaworotko, M. J. *J. Am. Chem. Soc.* **2008**, *130*, 1560.

(5) (a) An, J.; Shade, C. M.; Chengelis-Czegan, D. A.; Petoud, S.; Rosi, N. L. *J. Am. Chem. Soc.* **2011**, *133*, 1220. (b) Della, R. J.; Liu, D.; Lin, W. *Acc. Chem. Res.* **2011**, *44*, 957.

(6) (a) Kong, X.; Ren, Y.; Long, L.; Zheng, Z.; Huang, R.; Zheng, L. *J. Am. Chem. Soc.* **2007**, *129*, 7016. (b) Kong, X.; Wu, Y.; Long, L.; Zheng, L.; Zheng, Z. *J. Am. Chem. Soc.* **2009**, *131*, 6918. (c) Zhang, Y. B.; Zhang, W. X.; Feng, F. Y.; Zhang, J. P.; Chen, X. M. *Angew. Chem., Int. Ed.* **2009**, *48*, 5287. (d) Jiang, G.; Wu, T.; Zheng, S-T; Zhao, X.; Lin, Q.; Bu, X.; Feng, P. *Cryst. Growth Des.* **2011**, *11*, 3713−3716.

(7) (a) Wang, X. Q.; Dai, S. *Angew. Chem., Int. Ed.* **2010**, *49*, 6664. (b) Ma, Z.; Yu, J. H.; Dai, S. *Adv. Mater.* **2010**, *22*, 261. (c) Fei, H. H.; Rogow, D. L.; Oliver, S. R. J. *J. Am. Chem. Soc.* **2010**, *132*, 7202. (d) Fei, H. H.; Bresler, M. R.; Oliver, S. R. J. *J. Am. Chem. Soc.* **2011**, *133*, 11110. (e) Zheng, S. T; Wu, T.; Irfanoglu, B.; Zuo, F.; Feng, P.; Bu, X. *Angew. Chem., Int. Ed.* **2011**, *50*, 8034. (f) Zheng, S. T; Wu, T.; Zuo, F.; Chou, C. T; Feng, P.; Bu, X. *J. Am. Chem. Soc.* **2012**, *134*, 1934.

(8) (a) Zhao, B.; Chen, X. Y.; Cheng, P.; Liao, D. Z.; Yan, S. P.; Jiang, Z. H. *J. Am. Chem. Soc.* **2004**, *126*, 15394. (b) Zhang, M. B.; Zhang, J.; Zheng, S. T.; Yang, G. Y. *Angew. Chem., Int. Ed.* **2005**, *44*, 1385. (c) Luo, F.; Batten, S. R.; Che, Y.; Zheng, J. M. *Chem.—Eur. J.* **2007**, *13*, 4948. (d) Zhao, X. Q.; Zhao, B.; Wei, S.; Cheng, P. *Inorg. Chem.* **2009**, *48*, 11048. (e) Zhou, B.; Kobayashi, A.; Cui, H. B.; Long, L. S.; Fujimori, H.; Kobayashi, H. *J. Am. Chem. Soc.* **2011**, *133*, 5736. (f) Wang, X. Y.; Avendaño, C.; Dunbar, K. R. *Chem. Soc. Rev.* **2011**, *40*, 3213.

(9) (a) Garibay, S. J.; Stork, J. R.; Wang, Z.; Cohen, S. M.; Telfer, S. G. *Chem. Commun.* **2007**, 4881. (b) Chen, P. K.; Che, Y. X.; Zheng, J. M.; Batten, S. R. *Chem. Mater.* **2007**, *19*, 2162. (c) Mavrandonakis, A.; Klontzas, E.; Tylianakis, E.; Froudakis, G. E. *J. Am. Chem. Soc.* **2009**, *131*, 13410. (d) Chen, Y. B.; Kang, Y.; Zhang, J. *Chem. Commun.* **2010**, *46*, 3182.

(10) (a) Xie, Z.; Ma, L.; DeKrafft, K. E.; Jin, A.; Lin, W. *J. Am. Chem. Soc.* **2010**, *132*, 922. (b) Zhang, Y. J.; Liu, T.; Kanegawa, S.; Sato, O. *J. Am. Chem. Soc.* **2010**, *132*, 912. (c) Ryu, D. W.; Lee, W. R.; Lee, J. W.; Yoon, J. H.; Kim, H. C.; Koh, E. K.; Hong, C. S. *Chem. Commun.* **2010**, *46*, 8779. (d) Zhao, J. P.; Hu, B. W.; Zhang, X. F.; Yang, Q.; Fallah, M. S. E.; Ribas, J.; Bu, X. H. *Inorg. Chem.* **2010**, *49*, 11325. (e) Nayak, S.; Harms, K.; Dehnen, S. *Inorg. Chem.* **2011**, *50*, 2714.

(11) (a) Rodriguez-Albelo, L. M.; Ruiz-Salvador, A. R.; Sampieri, A.; Lewis, D. W.; Gómez, A.; Nohra, B.; Mialane, P.; Marrot, J.; Sécheresse, F.; Mellot-Draznieks, C.; Biboum, R. N.; Keita, B.; Nadjo, L.; Dolbecq, A. *J. Am. Chem. Soc.* **2009**, *131*, 16078. (b) Zhuang, G. L.; Chen, W. X.; Zhao, H. X.; Kong, X. J.; Long, L. S.; Huang, R. B.; Zheng, L. S. *Inorg. Chem.* **2011**, *50*, 3843. (c) Lu, Z. Z.; Zhang, R.; Li, Y. Z.; Guo, Z. J.; Zheng, H. G. *J. Am. Chem. Soc.* **2011**, *133*, 4172.

(12) (a) Rominger, F.; Müller, A.; Thewalt, U. *Chem. Ber.* **1994**, *127*, 797. (b) Nöth, H.; Sanudo, T. S. *Eur. J. Inorg. Chem.* **2002**, 602. (c) Cheng, Y.; Doyle, D. J.; Hitchcock, P. B.; Lappert, M. F. *Dalton. Trans.* **2006**, 4449. (d) Muryn, E. C.; Halliwell, C. A.; Timco, M. A.; Wernsdorfer, G. A.; Winpenny, W.; R. E. P.. *Chem. Commun.* **2007**, 801. (e) Mensinger, Z. L.; Gatlin, J. T.; Meyers, S. T.; Zakharov, L. N.; Keszler, D. A.; Johnson, D. W. *Angew. Chem., Int. Ed.* **2008**, *47*, 9484.

(13) PLATON VOIDS probe diameter 1.2 Å: Spek, A. L. *J. Appl. Crystallogr.* **2003**, *36*, 7.

(14) (a) Hayashi, H.; Côté, A. P.; Furukawa, H.; O'Keeffe, M.; Yaghi, O. M. *Nat. Mater.* **2007**, *6*, 501. (b) Park, K. S.; Ni, Z.; Côté, A. P.; Choi, J. Y.; Huang, R.; Uribe-Romo, F. J.; Chae, H. K.; O'Keeffe, M.; Yaghi, O. M. *Proc. Natl. Acad. Sci. U.S.A.* **2006**, *103*, 10186.

(15) (a) Caskey, S. R.; Wong-Foy, A. G.; Matzger, A. J. *J. Am. Chem. Soc.* **2008**, *130*, 10870. (b) Choi, H. S.; Suh, M. P. *Angew. Chem., Int. Ed.* **2009**, *48*, 6865. (c) Sumida, K.; Horike, S.; Kaye, S. S.; Herm, Z. R.; Queen, W. L.; Brown, C. M.; Grandjean, F.; Long, G. J.; Dailly, A.; Long, J. R. *Chem. Sci.* **2010**, *1*, 184. (d) Wu, H.; Reali, R. S.; Smith, D. A.; Trachtenberg, M. C.; Li, J. *Chem.—Eur. J.* **2010**, *16*, 13951.